Lagrangian modelling of reactive contaminant transport in the multi-component marine medium

Igor Brovchenko[a], Kyeong Ok Kim[b], Vladimir Maderich[a,*], Kyung Tae Jung[c], Katheryna Kovalets[a]

[a]Institute of Mathematical Machine and System Problems, Kyiv, 03187, Ukraine. 0000-0003-0576-351X; 0000-0003-3143-0727; 0000-0003-3027-4697.

[b]Marine Environmental Research Center, Korea Institute of Ocean Science and Technology, Busan 49111, Republic of Korea. 0000-0002-2066-9145

[c]Oceanic Consulting and Trading, Gangneung 25601, Republic of Korea. 0000-0002-4295-7092

Accepted manuscript *Computers and Geosciences*, 187, 105579. https://doi.org/10.1016/j.cageo.2024.105579

ARTICLE INFO

Keywords:

Particle-tracking method

Reactive radionuclides in ocean

Master equation

Water-sediment boundary conditions

Authorship contribution statement

Igor Brovchenko: Co-first authorship, Method conception, Algorithm development, Code writing, Manuscript writing.

Kyeong Ok Kim: Co-first authorship, Lagrangian simulation and processing; Manuscript review and writing

Vladimir Maderich: Design of the study, Funding acquisition. Transport equations, Test cases conception, Manuscript writing.

Kyung Tae Jung: Funding acquisition. Error analysis. Manuscript review and writing

Katheryna Kovalets: Analytical and Eulerian numerical solutions for section 4.2, Section 4.2 writing.

ABSTRACT

The particle-tracking method for transporting radionuclides in multicomponent ocean medium (water and multifractional suspended and deposited sediments) is considered using a probabilistic approach for simulating interaction processes between several states of radioactivity. The state transformations as a result of reactions of the first order were described using the master equation for the probability of the particle being in the given state. Transition probabilities between all possible states can be obtained from the numerical solution of the matrix master equation that is derived in the paper. In the first approximation, the Euler method was used to obtain a solution for the next time step. This approach can be applied to any linear system of equations describing phase transitions with any number of states, but it requires small values of the transition probabilities to ensure only a single-phase change during one time step. The paper also focuses on deriving the Lagrangian interface conditions between the water column and bottom deposition. To apply the probabilistic approach, the boundary conditions were considered as the reaction terms in a thin near-bottom interface layer in which boundary conditions were converted into source terms. For this layer, the corresponding master equation was derived to obtain transitional probabilities for particle states. The developed approaches were tested on numerical and analytical solutions of two test cases. It was found that the optimal thickness of the interface layer must be larger than the maximum vertical displacement of the particle during the one-time step, but it must be small enough to approximate the condition of uniform distribution of concentration in this layer.

1. Introduction

Lagrangian models or particle tracking models are widely used to simulate pollution transport in the marine environment (Lynch et al., 2014; van Sebille et al., 2018; Periáñez et al., 2019). In these models, the released amount of pollutant is represented by an ensemble of particles, each one equivalent to a given amount of pollutants being in different phases (e.g., in dissolved and particulate states). The Lagrangian approach leads to the integration of particle trajectories including random diffusion processes and particle phase changes. The particle methods may be much faster in comparison with the Eulerian models. Their usage can be simpler, being mass conservative, and enabling trajectory analysis. Methods of high-order trajectory integration are efficient and easy to use. However, the application of particle-tracking models becomes more complex in reactive environments, when there is a transfer between dissolved and particulate states and/or transfer of pollutants from one chemical form to another. These substances include many organic (e.g., PCB) and inorganic toxicants such as radionuclides and heavy metals (Chapra, 1997).

Here we restrict ourselves to reactions of first order considering radionuclides, many of which are significantly adsorbed by sediment particles (Periáñez et al., 2018) being, in turn, an important source of contamination in shallow seas (Brovchenko et al., 2022). Sorption processes can take place in two stages: a fast sorption during exclusively surface-level contact, and a slow sorption during the penetration of ions into the pores of sediment particles (Maderich et al., 2017; Periáñez et al., 2018). Radionuclides such as plutonium can exist in various chemical forms depending on the properties of the surrounding aquatic environment. The transport of radioactivity in the ocean is described by the Eulerian and Lagrangian models. The 3D generalized Euler model developed by (Maderich et al., 2017) describes the transport processes in the dissolved and multifraction solid phases in the water column and bottom sediments.

A Lagrangian method for the simulation of the dispersion of particle-reactive radionuclides in marine environment has been developed in a pioneering paper by Periáñez and Elliot (2002). A systematic comparison of the Eulerian and Lagrangian approaches is given by Periáñez et al. (2019) and Periáñez (2020). Computational aspects of Lagrangian modelling of the radionuclide transport were discussed by Periáñez et al. (2023). However, the general particle tracking approach describing the interaction of radionuclides in different states in the multifractional sediment has not been developed yet.

In this paper, the particle-tracking method for the transport of radionuclides in the marine environment is considered using a probabilistic approach for simulating processes of interaction between several states of activity. In

particular, we focus on the derivation of the interface conditions between the water column and bottom deposition. This paper is organized as follows: the equations of radionuclide transport are given in Section 2. The Lagrangian method is described in Section 3. Two test cases are considered in Section 4. Our findings are summarized in Section 5.

2. Methodology

Following Maderich et al. (2017), the Eulerian equations for concentration of the dissolved phase of radionuclides in the water column C_d^w [Bq m^{-3}], and the concentration on suspended sediments phase of radionuclides $C_{p,i}^w$ [Bq m^{-3}] for sediment size class *i* are written in Cartesian coordinates (x, y, z) as

$$\frac{\partial C_d^w}{\partial t} + \vec{U}\nabla C_d^w = -a_{ds}\left(C_d^w \sum_{i=0}^{n} S_{p,i} K_{d,i} - C_p^w\right) - \lambda C_d^w + F_{diff}\left(C_d^w\right) \quad (1)$$

$$\frac{\partial C_{p,i}^w}{\partial t} + \vec{U}\nabla C_{p,i}^w = W_{p,i}\frac{\partial C_{p,i}^w}{\partial z} + a_{ds}\left(C_d^w S_{p,i}^w K_{d,i}^w - C_{p,i}^w\right) - \lambda C_{p,i}^w + F_{diff}\left(C_{p,i}^w\right) \quad (2)$$

Here *t* is time [s];, *z* is vertical coordinate directed upward [m]; $\vec{U} = (U, V, W)$ are the meridional, zonal and vertical velocity vectors [m s^{-1}]; $\vec{\nabla}$ is the 3D vector operator; i is a sediment size class index; $n+1$ is the total number of sediment fractions; $S_{p,i}$ is the concentration of *i*-th class of suspended sediment [kg m^{-3}]; $W_{p,i}$ is directed downward settling velocity of sediment class *i* [m s^{-1}]; a_{ds} is the desorption rate [s^{-1}]; $K_{d,i}$ is the distribution coefficient [m^3 kg^{-1}]; λ is the radionuclide decay rate [s^{-1}]. Note that for simplicity, equations (1)-(2) do not take into account the slow processes of exchange between particulate matter and water (Maderich et al., 2017; Periáñez et al., 2018) and the presence of various chemical forms of the element (Maderich et al., 2022).

The distribution of radionuclides in the bottom is described within the simplified framework of a single well-mixed layer proposed by Maderich et al. (2017). The equations for the layer averaged concentration of particulate phase of radionuclide $C_{s,i}^b$ [Bq kg^{-1} of sediments] for sediment size class *i* in the bottom layer, and for the layer averaged concentration of radionuclide in the pore water C_d^b [Bq m^{-3}] are

$$\frac{\partial Z_* \phi_i C_{s,i}^b}{\partial t} = a_{bds} Z_* \left(K_{d,i} C_d^w - C_{s,i}^b \right) + a_{rs} Z_* \left(\hat{C}_s^b \frac{K_{d,i}}{\hat{K}_d^b} - C_{s,i}^b \right) + \frac{D_i C_{p,i}^w}{\sigma \rho_{s,i} S_{p,i}} - \frac{E_i C_{s,i}^b}{\sigma \rho_{s,i}} - \lambda Z_* C_{s,i}^b, \tag{3}$$

$$C_d^b = \frac{W_{pw} C_d^w(-H) + a_{ds} \theta Z_* \sigma \hat{C}_s^b}{W_{pw} + a_{ds} \theta Z_* \sigma \hat{K}_d^b}, \tag{4}$$

where

$$a_{bds} = \frac{a_{ds} \theta W_{pw}}{W_{pw} + a_{ds} \theta Z_* \sigma \hat{K}_d^b},$$

$$a_{rs} = \frac{a_{ds}^2 \theta^2 Z_* \sigma \hat{K}_d^b}{W_{pw} + a_{ds} \theta Z_* \sigma \hat{K}_d^b}.$$

Here D_i and E_i are sediment deposition and erosion rates, respectively [kg m^{-2}s^{-1}]; Z_* is the thickness of the single layer of sediment [m]; ϕ_i is the fraction of particles of *i*-th class in the bottom sediment ($\sum_{i=0}^{n} \phi_i = 1$); ε is a constant porosity in the layer; $\rho_{s,i}$ is the density of the sediments of *i*-th class [kg m^{-3}]; θ is a correction factor that takes into account that part of the sediment particle surface may be hidden by other sediment particles; $C_d^w(-H)$ is a near-bottom value of C_d^w at $z = -H$; W_{pw} is an exchange rate between bottom and water column [m s^{-1}], $W_{pw} = 0.1778 u_* \mathrm{Re}^{-0.2} \mathrm{Sc}^{-0.604}$ (Boudreau, 1997); $\mathrm{Re} = \delta_* u_* / \nu_D$ is the Reynolds number; δ_* is an average height of the roughness elements; $\mathrm{Sc} = \nu_M / \nu_D$ is the Schmidt number; ν_M is kinematic viscosity [m^{2}s^{-1}]; ν_D is molecular diffusivity [m^{2}s^{-1}]. The friction velocity u_* is calculated using the near-bottom horizontal velocity at a distance Δh from the bottom, as

$$u_* = \frac{\kappa}{\ln(\Delta h / z_0)} \sqrt{U^2 + V^2},$$

where z_0 is the roughness parameter, $\kappa = 0.4$ is the von Kármán constant.

The total concentration of the particulate phase of radionuclide C_p^w in suspended sediments and bed sediments $\hat{C}_s^b$ are, respectively

$$C_p^w = \sum_{i=0}^{n} C_{p,i}^w,\ \hat{C}_s^b = \sum_{i=0}^{n} \rho_{s,i}\phi_i C_{s,i}^b,$$

whereas the weighted nondimensional distribution coefficient is

$$\hat{K}_d^b = \sum_{i=0}^{n} \rho_{s,i}\phi_i K_{d,i},$$

The turbulent diffusion terms are written as

$$F_{diff}(x) = \frac{\partial}{\partial z} K_V \frac{\partial(x)}{\partial z} + \vec{\nabla}_H K_H \vec{\nabla}_H (x),$$

where K_V and K_H are vertical and horizontal eddy diffusivity, respectively [$m^2\ s^{-1}$], $\vec{\nabla}_H$ is the horizontal vector operator. Following Periáñez et al. (2018), the dependence $K_{d,i}$ on sediment particle diameter d_i [m] and the exchange velocity χ [$m\ s^{-1}$] is

$$K_{d,i} = \frac{\chi}{a_{ds}} \frac{6}{d_i}. \tag{5}$$

At the ocean surface the boundary conditions for (1)-(2) are:

$$K_V \frac{\partial C_d^w}{\partial z} - W C_d^w = -q_d, \tag{6}$$

$$K_V \frac{\partial C_{p,i}^w}{\partial z} + (W - W_{p,i}) C_{p,i}^w = -q_{p,i}, \tag{7}$$

where q_d and $q_{p,i}$ are atmospheric deposition fluxes [$Bq\ m^{-2}\ s^{-1}$]. The boundary conditions on the bottom at $z = -H + z_0$ are

$$K_V \frac{\partial C_d^w}{\partial z} = W_{pw}\left(C_d^w - C_d^{\,b}\right), \tag{8}$$

$$W_{p,i} C_{p,i}^w + K_V \frac{\partial C_{p,i}^w}{\partial z} = C_{s,i}^b E_i + \frac{D_i}{S_{p,i}} C_{p,i}^w. \tag{9}$$

The Exner equation for changes in bed layer thickness due to erosion and deposition of sediments and equations for variations of sediment fractions have been supplemented to the system of equations following Maderich et al. (2017). The deposition and erosion rates for a mixture of non-cohesive and cohesive sediments are described by relations given by Maderich et al. (2017). The settling velocity $W_{p,i}$ for non-cohesive fractions of sediments is calculated

according to van Rijn (1984). For cohesive fraction, settling velocity is corrected for flocculation following (Winterwerp, van Kesteren, 2004).

3. Lagrangian algorithm

3.1. Transport equations

In Lagrangian radionuclide transport models, the released activity is represented by many particles with an equal amount of activity (Bq). These particles can possess several states: dissolved in the water column, adsorbed on suspended sediment of a particular size, dissolved in the pore water, and adsorbed on the bed sediments of a particular size. Note that in this model, the concentration of radionuclides in the pore water is in equilibrium with the concentration in the bottom sediments. If there are $n+1$ sediment size classes then we have $N=1+2(n+1)$ the total states of the dissolved and particulate radionuclides.

In general form equations (1)-(3) can be rewritten as

$$\frac{\partial C_\alpha}{\partial t} = -\frac{\partial u_{\alpha,k} C_\alpha}{\partial x_k} + \frac{\partial}{\partial x_k} K_{kl}^\alpha \frac{\partial C_\alpha}{\partial x_l} + \sum_{\beta=1}^{N} r_{\alpha\beta} C_\beta, \ \alpha = \overline{1,N}, \tag{10}$$

where C_α (Bq m^{-3}) is the concentration of material in the state α, and $r_{\alpha\beta}$ are the kinetic coefficients of the first-order reaction terms in the α - th state, $u_{\alpha,k}$ includes settling velocity for sediment particles,

$$K_{kl}^\alpha = \begin{pmatrix} K_H^\alpha & 0 & 0 \\ 0 & K_H^\alpha & 0 \\ 0 & 0 & K_V^\alpha \end{pmatrix}. \tag{11}$$

Eq. (10) can be considered as the Fokker-Planck equation for the particle location probability density function p_α [m^{-3}] in the state α:

$$\frac{\partial p_\alpha}{\partial t} = -\frac{\partial u_{\alpha,k}^{(drift)} p_\alpha}{\partial x_k} + \frac{\partial^2 K_{kl}^\alpha p_\alpha}{\partial x_k \partial x_l} + \sum_{\beta=1}^{N} r_{\alpha\beta} p_\beta, \quad \alpha = \overline{1,N}, \tag{12}$$

where $u_{\alpha,k}^{(drift)} = u_{\alpha,k} + \partial K_{kl} / \partial x_l$. At initial time moment the concentration in particle location can be represented as delta-function. Then equation (12) can be derived using the relation

$$C_\alpha = m p_\alpha(x,y,z,t), \tag{13}$$

where m is the amount of radioactivity [Bq] in the particle. For the ensemble of particles, the total concentration is derived by summing the contributions into the concentration from every particle.

The probability distribution of the initial particle location is also the delta function. Evolution in time of the probability $P_\alpha(t)$ of the particle being in the $\alpha-$th state can be described using the master equation

$$\frac{\partial P_\alpha}{\partial t} = \sum_{\beta=1}^{N} r_{\alpha\beta} P_\beta, \quad \alpha = \overline{1,N}. \tag{14}$$

where

$$P_\alpha(t) = \iiint_{\pm\infty} p_\alpha(\tilde{x},\tilde{y},\tilde{z},t)d\tilde{x}d\tilde{y}d\tilde{z}. \tag{15}$$

It was obtained by integrating (12) by volume of a plume of probability density. It was assumed that kinetic coefficients slowly vary in space comparatively with the size of the plume of probability at the time step Δt. In the general case, a system of equations (14) for *N* states can be solved numerically. Equations (14) can be also written in the matrix form as

$$\frac{d\mathbf{P}}{dt} = \mathbf{RP}, \tag{16}$$

where $\mathbf{P} = (P_1, P_2, \ldots P_N)^T$, $\mathbf{R} = r_{\alpha\beta}$ $(\alpha = \overline{1,N}, \quad \beta = \overline{1,N})$. A vector of initial conditions is $\mathbf{P}_0 = \mathbf{P}(0) = (P_1(0), P_2(0), \ldots P_N(0))^T$. If the initial state of the particle is α then $P_\alpha = 1, \quad P_\beta = 0, \ (\beta = \overline{1,N}, \quad \beta \neq \alpha)$. Using the first-order numerical approximation for the solution of the equations (14) or (16) and assuming that $\left|r_{\alpha\beta}\right|\Delta t << 1$. we obtain the solution as

$$\mathbf{P}(\Delta t) = \mathbf{RP}_0 \Delta t, \tag{17}$$

$$P_\alpha(\Delta t) = 1 + r_{\alpha\alpha}\Delta t, \quad P_\beta(\Delta t) = r_{\alpha\beta}\Delta t \ \text{ at } \ \alpha \neq \beta. \tag{18}$$

The approach (17)-(18) can be applied to any linear system of equations describing phase transitions with any number of states. Generally, a particle can change its state several times during a finite period. A requirement of small $r_{\alpha\beta}\Delta t$ is used to ensure only a single phase change occurs during one time step (Kinzelbach, 1987). In the case of fast kinetic reactions, solving (14) or (16) may require higher-order numerical schemes or smaller time steps. The particle tracking method, based on the method of moments (Maderich et al., 2021), has lower time step limitations. In this approach, the system of equations for the first three moments includes an equation for the zero-order moment, extending the

master equation (14), first and second-order moment equations. However, the numerical solution of the full system of equations for multiple states in the 3D domain requires large computational load comparatively with simple method proposed in this study.

Evolution of the particle position in the state α during the time step Δt consists of deterministic displacement due to currents, inhomogeneity of diffusion coefficient, and displacement by an uncorrelated random walk:

$$\begin{aligned} x_\alpha(t+\Delta t) &= x_\alpha(t) + \left(U_\alpha + \frac{\partial K_H^\alpha}{\partial x} \right) \Delta t + \xi_x \sqrt{2K_H^\alpha \Delta t}, \\ y_\alpha(t+\Delta t) &= y_\alpha(t) + \left(V_\alpha + \frac{\partial K_H^\alpha}{\partial y} \right) \Delta t + \xi_y \sqrt{2K_H^\alpha \Delta t}, \\ z_\alpha(t+\Delta t) &= z_\alpha(t) + \left(W_\alpha + \frac{\partial K_V^\alpha}{\partial z} \right) \Delta t + \xi_z \sqrt{2K_V^\alpha \Delta t}, \end{aligned} \tag{19}$$

where U_α, V_α and W_α are velocity components on coordinate axis (x, y, z) for state α; ξ_x, ξ_y, ξ_z are the normally distributed random variables with zero mean value and unit variance $\xi_i = N(0,1)$.

The particle tracking process for passive tracers does not depend on the rest of the particles. Therefore, the computation can be parallelized using the MPI library when tracking for a given number of particles is performed independently, whereas the outputs of all processes are summarized to get the total results. This approach works well when Eulerian data necessary for particle tracking (velocity, diffusivity, etc.) can be placed in processor memory. Otherwise, I/O-enhancing techniques are needed to accelerate computations (Kehl et al., 2023).

If the number of particles in the bed layer grid element is much greater than the number of particles suspended in the water grid element, the particle-tracking algorithm may be inefficient. Most of the particles are in the bottom sediment layer, they do not move, they have the same properties, and they are placed in the same grid element, but they all require using an algorithm for calculating probabilities at each time step for each particle. Such a situation may arise, for example, in the problem of secondary contamination of a water column from a previously contaminated bottom. As will be shown in section 4.2, in this case, the number of particles in the water column may be 100 times smaller than in the bed layer, and almost the entire computational resource will be spent on motionless bottom particles. Therefore, for such a case, the algorithm was optimized. We did not store all bottom particles in memory but treated them as one, storing only the total number of particles in a grid element instead of a large array. The transitional probabilities were calculated once for all bottom particles in the grid element and then the number of particles that should appear in other states is calculated. For the problem considered in section 4.2, this approach made

it possible to speed up the runtime of the numerical solution of the problem up to 100 times exploiting the fact that the majority of particles are not moving inside the bottom layer and therefore were excluded from calculation.

3.2. Bottom boundary conditions

To satisfy bottom boundary conditions (8)-(9) written in the form of fluxes we need to adapt the Lagrangian algorithm for this aim. Fluxes through the bed surface in terms of Lagrangian particles correspond to changing of a particle state from 'dissolved in the water column' to 'dissolved in pore water' and from the 'adsorbed on suspended sediment state' to the 'state of adsorbed on settled sediment on the bed' or vice versa. Therefore, boundary conditions were considered as reaction terms in transport equations. To satisfy them the correct probabilities should be estimated. For this purpose, we introduced a thin near-bottom interface layer of thickness ΔZ where boundary conditions (8)-(9) are converted into source terms which are uniformly distributed in the interface layer of thickness ΔZ . Then equations (1)-(2) take the form:

$$\frac{\partial C_d^w}{\partial t} + \vec{U}\nabla C_d^w = -a_{ds}\left(C_d^w \sum_{i=0}^{n} S_{p,i} K_{d,i} - C_p^w\right) - \lambda C_d^w + \frac{\partial}{\partial z} K_V \frac{\partial C_d^w}{\partial z} - H(z)\left[\frac{Z_*}{\Delta Z} a_{bds}\sigma\left(\hat{K}_d^b C_d^w(-H) - \hat{C}_d^b\right)\right], \tag{20}$$

$$\frac{\partial C_{p,i}^w}{\partial t} + \vec{U}\nabla C_{p,i}^w = W_{p,i}\frac{\partial C_{p,i}^w}{\partial z} + a_{ds}\left(C_d^w S_{p,i}^w K_{d,i}^w - C_{p,i}^w\right) - \lambda C_{p,i}^w + \frac{\partial}{\partial z} K_V \frac{\partial C_{p,i}^w}{\partial z} - H(z)\left[\frac{W_{p,i} C_{p,i}^w(-H)}{\Delta Z} - \frac{E_i C_{s,i}^b}{\Delta Z}\right], \tag{21}$$

where the Heaviside function is $H(z) = 1$ in the interface layer of thickness ΔZ , and $H(z) = 0$ outside this layer. By introducing the source terms in (20)-(21) we change the bottom boundary conditions (8)-(9) to a zero flux conditions:

$$K_V \frac{\partial C_d^w}{\partial z} = 0, \qquad W_{p,i} C_{p,i}^w + K_V \frac{\partial C_{p,i}^w}{\partial z} = 0. \tag{22}$$

In the particle random walk algorithm, particles of any state reflect from the bottom surface if they cross it during the time step.

To obtain the master equation for the state probabilities in the interface layer, we integrated the equations (20)-(21) over the thickness of the interface layer and used (3) for the bed layer which yields

$$\frac{\partial P_W}{\partial t} = -a_{ds}\left(P_W \sum_{i=0}^{n} S_{p,i} K_{d,i} - \sum_{i=0}^{n} P_{P,i}\right) - a_{bds}\left(\frac{Z_*}{\Delta Z}\sigma \hat{K}_d^b P_W - \sum_{i=0}^{n} P_{B,i}\right) - \lambda P_W, \quad (23)$$

$$\frac{\partial P_{P,i}}{\partial t} = a_{ds}\left(P_W S_{p,i}^w K_{d,i}^w - P_{P,i}\right) - \frac{W_{p,i} P_{P,i}}{\Delta Z} + \frac{E_i P_{B,i}}{Z_* \phi_i \rho_s \sigma} - \lambda P_{P,i}, \quad (24)$$

$$\frac{\partial P_{B,i}}{\partial t} = a_{bds}\left(\rho_s \phi_i \sigma \frac{Z_*}{\Delta Z} K_{d,i}^b P_W - P_{B,i}\right) + a_{rs}\left(\rho_s \phi_i \frac{K_{d,i}^b}{\hat{K}_d^b} \sum_{i=0}^{n} P_{B,i} - P_{B,i}\right) + \frac{W_{p,i} P_{P,i}}{\Delta Z} - \frac{E_i P_{B,i}}{Z_* \phi_i \rho_s \sigma} - \lambda P_{B,i}. \quad (25)$$

Here P_W is a probability for a particle to be in a dissolved state in the near bottom layer, $P_{P,i}$ is a probability for a particle to be absorbed on suspended sediments of class *i* in the interface layer, $P_{B,i}$ is a probability for a particle to be in absorbed on bed sediments of class *i* in the bed layer. When deriving the equations (24)-(25), it is assumed that ϕ_i slowly changes in time, so that ϕ_i can be considered constant per time step.

We set the initial probability vector of the current particle state on each time step. For the particle state α we set $P_\alpha(0) = 1$, whereas other probabilities set to 0. Here α represents the possible state of the particle: *W* for dissolved state, S_i for particulate state, and B_i for the bottom. Then according to (16) a new vector of probability distribution $\mathbf{P}(\Delta t)$ on the next time step is calculated. This vector defines the transition probabilities from the previous state α to other possible states (including α) on the next time step. Applying this algorithm to equations (23)-(25) we can calculate the transition probabilities for all particle states as shown in Fig.1:

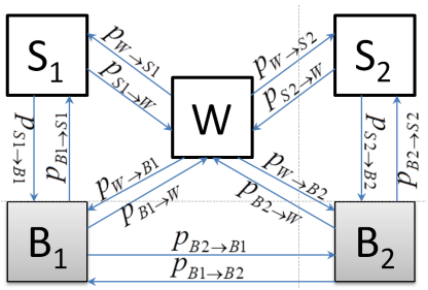

Figure 1: Scheme of transitional probabilities in interface layer for particle states: dissolved state (*W*), and two particulate states of suspended sediment (S_i) and bed layer (B_i).

- A particle in the dissolved state (*W*) in the interface layer may go to the bed sediments with probability $p_{W\to B} = (Z_* / \Delta Z) a_{bds} \sigma \hat{K}_d^b \Delta t$ or go in adsorbed on suspended sediments state with probability $p_{W\to S} = a_{ds} \sum_{i=0}^{n} S_{p,i} K_{d,i} \Delta t$ or stay dissolved with probability $p_{W\to W} = 1 - p_{W\to B} - p_{W\to S}$.

- A particle in the adsorbed on suspended sediments of class *i* state (S_i) in the near bottom layer particle may settle down to the bed sediments with probability $p_{Si\to Bi} = (W_{p,i} / \Delta Z)\Delta t$ or go to the dissolved in the water column state with probability $p_{Si\to W} = a_{ds} S_{p,i} K_{d,i} \Delta t$ or stay in the current state with probability $p_{Si\to Si} = 1 - p_{Si,W} - p_{Si,Bi}$.

- A particle in the adsorbed on bed sediments of class *i* state (B_i)in the bed layer may be eroded to the suspended sediments with probability $p_{Bi\to Si} = (E_i \Delta t) / (\phi_i \rho_s \sigma Z_*)$ or to go to the dissolved state in the interface layer with probability $p_{B\to W} = a_{bds} \Delta t$ or to go to other fraction *j* of bed sediments with probability $p_{Bi\to Bj} = a_{rs} \rho_s \varphi_i (K_{d,j} / \hat{K}_d^b) \Delta t$ or to stay in the current state with probability $p_{Bi\to Bi} = 1 - p_{Bi\to Si} - p_{B\to W} - \sum_{j=0}^{n} p_{Bi\to Bj}$.

After the calculation of all possible transition probabilities $p_{\alpha\to\beta}$ from the current state α, we generate the uniformly distributed random number *r* to select the new state β for the particle on the next time step. For this, the probability distribution $F_{\alpha\to\beta}(\beta)$ was calculated from the density distribution $p_{\alpha\to\beta}(\Delta t)$ as

$$F_{\alpha\to\beta}(\beta) = \sum_{\alpha=1}^{\beta} P_{\alpha\to\beta}, \tag{25}$$

where $F_{\alpha\to 1} = P_{\alpha\to 1}$ and $F_{i\to N} = 1$. Then we generate the random number r in the interval [0,1] and define the index of the new state from the inequality

$$F_{\alpha\to\beta-1} < r < F_{\alpha\to\beta}. \tag{26}$$

The consequent steps of the algorithm for the interface layer are shown in Fig. 2:

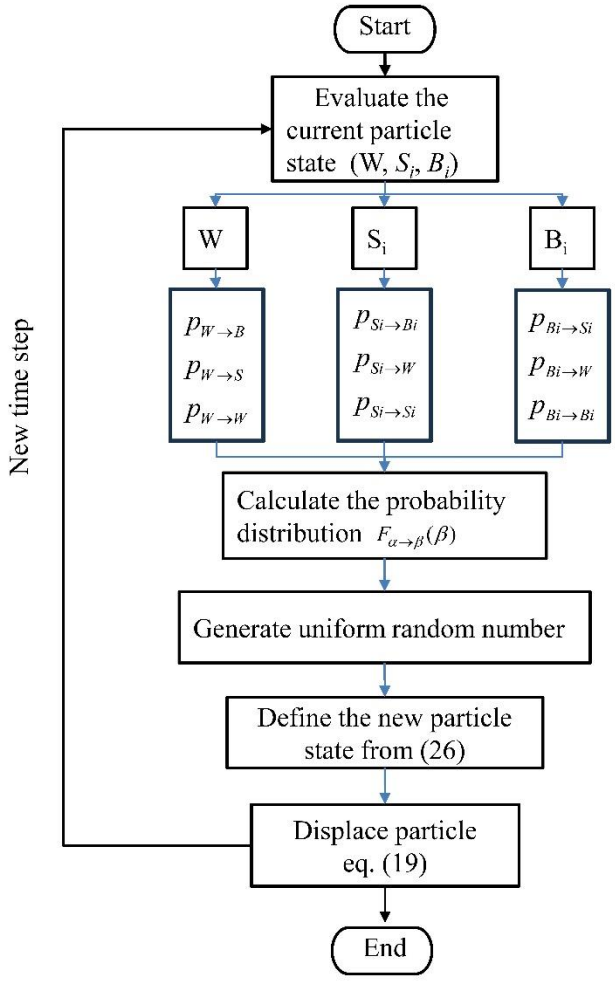

Figure 2: Flowchart of particle transitions and displacement in the interface layer.

The interface layer's minimum thickness is chosen to be greater than the characteristic displacement of the particle and much less than the characteristic thickness of the bottom boundary layer. An example of such an analysis is given in section 4.2.

4. Particular cases

4.1. Adsorption on multifraction suspended sediments

Consider the cubic box filled with water contaminated by ^{134}Cs in the presence of uniformly mixed suspended sediments of three non-cohesive fractions with uniform concentration $S_{p,i}$. The initial concentration is assumed to be $C_d^w(0) = 1$ Bq m^{-3}. Initially suspended sediments are clean of radioactive material: $C_{p,i}(0) = 0$. There is no exchange with the bed. The system of equations for spatially uniform concentrations in dissolved and particulate forms is

$$\begin{cases} \dfrac{\partial C_d^w}{\partial t} = -a_{ds}\left(C_d^w \sum_{i=1}^{n} S_{p.i} K_{d,i} - C_p^w \right) - \lambda C_d^w, \\ \dfrac{\partial C_{p,i}^w}{\partial t} = a_{ds}\left(C_d^w S_{p.i} K_{d,i} - C_{p,i}^w \right) - \lambda C_{p,i}^w, \qquad i = \overline{1,n.} \end{cases} \tag{27}$$

The corresponding system of ordinary differential equations for the probabilities P_α is

$$\begin{cases} \dfrac{\partial P_1}{\partial t} = -r_{11} P_1 + r_{12} \sum_{i=0}^{n} P_{2i} - r_{13} P_1, \\ \dfrac{\partial P_{2,i}}{\partial t} = r_{21,i} P_1 - r_{22} P_{2i} - r_{23} P_{2i}, \qquad i = \overline{1,n} \\ \dfrac{\partial P_3}{\partial t} = r_{33}\left(P_1 + \sum_{i=0}^{n} P_{2i} \right), \end{cases} \tag{28}$$

where $r_{11} = a_{ds} \sum_{i=1}^{n} S_{p,i} K_{d,i}$, $r_{21,i} = a_{ds} S_{p,i} K_{d,i}$, $r_{12} = r_{22} = a_{ds}$, $r_{13} = r_{23} = \lambda$. The state indices of α reflect the following correspondence: $\alpha = 1$ are particles in the dissolved state, $\alpha = 2$ are particles interacting with the sediment fraction of fraction i, and $\alpha = 3$ are particles in the decayed state.. Initial conditions at *t*=0 are

$P_1(0) = P_{00}$, $P_{2i}(0) = P_{i0}$, $P_3(0) = 0$, $\sum_{i=1}^{n} P_{i0} = P_{s0}$. The analytical solution of (28) is

$$\begin{aligned} P_1(t) &= \frac{r_{12}}{r_{11} + r_{12}} \left(\frac{r_{11} P_{00} - r_{12} P_{s0}}{r_{12}} \exp\left[-(r_{11} + r_{12} + r_{13}) t \right] + (P_{00} + P_{s0}) \exp(-r_{13} t) \right), \\ P_{2,i}(t) &= \frac{r_{21,i}}{r_{11} + r_{12}} \left(\frac{-r_{11} P_{00} + r_{12} P_{s0}}{r_{11}} \exp\left[-(r_{11} + r_{12} + r_{13}) t \right] + (P_{00} + P_{s0}) \exp(-r_{13} t) \right) \\ &+ \left(P_{i0} + \frac{r_{21,i}}{r_{12}} P_{s0} \right) \exp(-(r_{13} + r_{11}) t), \\ P_3(t) &= 1 - \exp(-r_{13} t). \end{aligned} \tag{29}$$

The approximate first-order solutions of equations (28) are

$$P_1(\Delta t) = a_{ds} \Delta t, \quad P_{2,i}(\Delta t) = a_{ds} S_i K_{d,i}^w \Delta t, \quad P_3(\Delta t) = \lambda \Delta t. \tag{30}$$

The simulations are carried out for 3 fractions of sediments (d_1=0.03 mm; d_2=0.125 mm; d_3=0.5 mm) with an equal concentration of each fraction $S_{p,i} = 0.2$ kg m^{-3}. The radionuclide was ^{134}Cs for which decay constant $\lambda = 1.02 \times 10^{-8}$ s^{-1}. The parameters of ^{134}Cs are $\chi = 3.8 \times 10^{-8}$ m s^{-1}, $a_{ds} = 1.16 \cdot 10^{-5}$ s^{-1} (Periáñez et al., 2018). The values of K_d are calculated using (5) for each fraction as $K_{d1} = 7$, $K_{d2} = 1.7$, $K_{d2} = 0.5$ m^{3}kg^{-1}. In this simulation,

we use 10 000 particles. The dependence of the probability P_2 on the non-dimensional time step $a_{ds}S_iK_{d,i}^w\Delta t$ according to the solution (29) is compared with the first-order solution (30) in Fig. 3a. As seen in the figure, if the product $a_{ds}S_{p,i}K_{d,i}\Delta t << 1$ then the first-order solution of (28) describes the exact solution well. In the simulation, $\Delta t = 120$ s results in the value of $a_{ds}S_{p,i}K_{d,i}\Delta t = 0.0017$. The accuracy and therefore time step can be increased by using higher-order schemes to solve the system of equations (28). System (27) is a system of linear ordinary differential equations which can be solved analytically in the same way as (28). Figure 3b compares the results of calculations using analytical formulas with calculations in the probabilistic approach. A comparison of simulation using first-order approximation (30) and analytical solutions for system equations (27) showed good agreement.

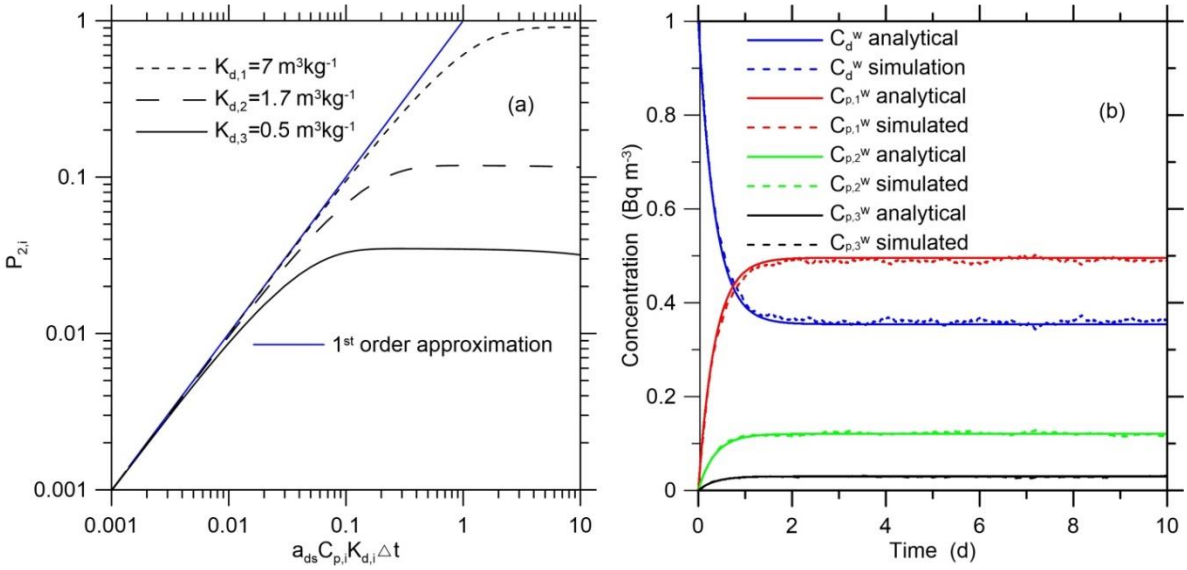

Figure 3: The dependence of the probability P_2 on the non-dimensional time step $a_{ds}S_iK_{d,i}^w\Delta t$ according to the solution (27) vs the first-order solution (a); Analytical solution of system equations for concentrations (27) vs numerical Lagrangian solution (b).

4.2. Bottom boundary layer formation due to the scavenging process

In the ocean, the scavenging of particle-reactive element results in the removal of this element from the water (Maderich et al., 2021). A well-known example is the scavenging of plutonium isotopes ^{239,240}Pu deposited on the

ocean surface as a result of nuclear tests (Livingstone et al., 2001). One of the observed phenomena was the formation of a long-lived layer of water with an increased concentration near the bottom. This was interpreted as a result of the tropospheric fallout from the Marshall Islands nuclear tests, for which contamination was more rapidly removed from surface waters into the bottom than from global fallout (Buesseler, 1997). Therefore, consider a special case of initially contaminated bottom sediment layer under the clean water column with sinking suspended sediment. The near-bottom layer of water is contaminated as a result of the diffusion from the bed sediments. Adsorption on suspended particles leads to the settling of radioactivity towards the bottom. Finally, the quasi-equilibrium concentration in water, suspended sediments, and bed sediments is established (Fig. 4).

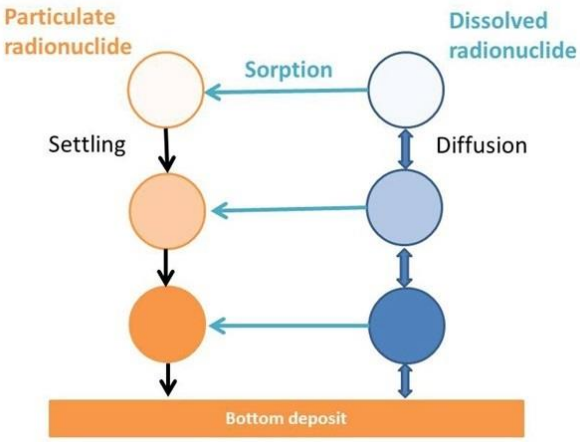

Figure 4: Sketch of contaminated bottom boundary layer. The colour intensity corresponds to the concentration of radionuclide.

For simplicity, consider the formation of a contaminated layer over the bottom for a single class of sinking non-cohesive sediment and a constant diffusivity. The deposition rate is $D_i = W_{p,i} S_{p,i}(-H)$. The decay of radioactivity and the bed layer's thickness change due to the particulate matter settling are ignored. The corresponding equilibrium equations (1)-(3) at $t \to \infty$ for C_d^w, C_p^w and C_s^b are

$$0 = -a_{ds}\left(C_d^w S_p K_d - C_p^w\right) + K_V \frac{\partial^2 C_d^w}{\partial z^2}, \tag{31}$$

$$0 = W_p \frac{\partial C_p^w}{\partial z} + a_{ds}\left(C_d^w S_p^w K_d^w - C_p^w\right) + K_V \frac{\partial^2 C_p^w}{\partial z^2}, \tag{32}$$

$$0 = a_{bds} Z_* \left(K_d^b C_d^w(-H) - C_s^b \right) + \frac{W_p C_p^w(-H)}{\rho_s (1-\varepsilon)}. \tag{33}$$

The equations (31)-(33) can be rewritten as single equation for C_d^w

$$K_v \left(K_v \frac{d^4 C_d^w}{d\tilde{z}^4} + W_p \frac{d^3 C_d^w}{d\tilde{z}^3} - (k_1 + k_2) \frac{d^2 C_d^w}{d\tilde{z}^2} \right) - k_1 W_p \frac{dC_d^w}{d\tilde{z}} = 0, \tag{34}$$

where $\tilde{z} = z + H$, $k_1 = a_{ds} S_p K_d$, $k_2 = a_{ds}$. Boundary conditions at $\tilde{z} = 0$ can be rewritten as

$$k_2 K_V \frac{\partial C_d^w}{\partial \tilde{z}} + W_p \left(k_1 C_d^w - K_V \frac{\partial^2 C_d^w}{\partial \tilde{z}^2} \right) = 0, \tag{35}$$

$$K_V \frac{\partial^3 C_d^w}{\partial \tilde{z}^3} - k_1 \frac{\partial C_d^w}{\partial \tilde{z}} = 0. \tag{36}$$

At a great distance from the bottom, the concentration of contamination decay

$$\tilde{z} \to \infty : \; C_d^w, \frac{\partial C_d^w}{\partial \tilde{z}}, \frac{\partial^2 C_d^w}{\partial \tilde{z}^2}, \frac{\partial^3 C_d^w}{\partial \tilde{z}^3} \to 0. \tag{37}$$

The equations (31)-(33) are completed by integral conservation law

$$\int_0^\infty C_d^w d\xi + \int_0^\infty C_p^w d\xi + \varepsilon C_d^b Z_* + (1-\varepsilon) \hat{C}_s^b Z_* = I_0, \tag{38}$$

where I_0 [Bq m^{-2}] is the initial value of bed layer contamination.

Define non-dimensional variables as

$$C_* = \frac{C_d^w z_o}{I_0}, \; z_* = \frac{\tilde{z}}{l_0},$$

where

$$l_0 = \frac{K_V (k_1 + k_2)}{k_1 W_p}.$$

Then equation (34) in non-dimensional form can be rewritten as

$$\mu \frac{d^4 C_*}{dz_*^4} + \gamma \frac{d^3 C_*}{dz_*^3} - \frac{d^2 C_*}{dz_*^2} - \frac{dC_*}{dz_*} = 0, \tag{39}$$

where

$$\mu = \frac{k_1^2 W_p^2}{K_V (k_1 + k_2)^3}, \; \gamma = \frac{k_1 W_p^2}{K_V (k_1 + k_2)^2}.$$

The characteristic values of the parameters for ^{239,240}Pu were $K_d = 100$ m^3 kg^{-1}, $a_{ds} = 1.16 \cdot 10^{-5}$ s^{-1} (Periáñez et al., 2018) whereas the parameters of the marine environment following Maderich et al. (2021) were $K_V = 10^{-4}$ m^2 s^{-1},

$S_p = 0.00025\,\mathrm{kg\ m^{-3}}$, $H = 4000$ m, $W_p = 5\cdot 10^{-5}\,\mathrm{m\ s^{-1}}$, $W_{pw} = 10^{-5}\,\mathrm{m\ s^{-1}}$, $\varepsilon = 0.6$, $Z_* = 0.05$ m. The corresponding values of parameters are $l_0 = 82\,\mathrm{m}$, $\mu = 1.25\cdot 10^{-3}$, $\gamma = 0.051$. As $\mu \to 0$ the solution of the reduced equation which satisfies the asymptotic conditions (37) is

$$C_* = A\exp(-z_*). \tag{40}$$

To satisfy boundary conditions (35)-(36) the thin boundary sublayer of thickness $O(\mu^{1/2})$ and amplitude $O(\mu^{1/2})$ should be added. In the first approximation, the terms $O(\mu^{1/2})$ can be ignored. Then the constant *A* can be found using conservation law. It is given in Appendix A. This solution can be compared with the numerical solution of the 1D version of equations (1)-(3) at $t \to \infty$ obtained using the Lagrangian approach and Eulerian Lax-Wendroff method (Fletcher, 1991). The initial amount of ^{239,240}Pu was I_0=0.5 Bq m^{-2}, the rest of the parameters are the same as given for the analytic solution. The Eulerian spatial and time steps were $\Delta z = 2$ m and $\Delta t = 500$ s, respectively. The comparison of analytic stationary solutions for dissolved and particulate concentration with corresponding profiles obtained at large times by using the Eulerian and Lagrangian numerical methods is given in Fig. 5. The concentration in the Lagrangian approach was calculated by the box-counting method using the box of 2 m length. This length was chosen for visualization purpose to be small enough to reproduce the structure of the solution and not too small to be noisy.

As can be seen in the figure, the results of numerical simulation of the nonstationary problem at large times by both methods are in good agreement with the analytical solution. Both numerical methods resolve the bottom boundary sublayer. Note that out of the total number of particles (1 million), only 1.5% were in the water. This example illustrates the usefulness of the approach proposed in Section 3.3, which made it possible to reduce the calculation time by two orders of magnitude.

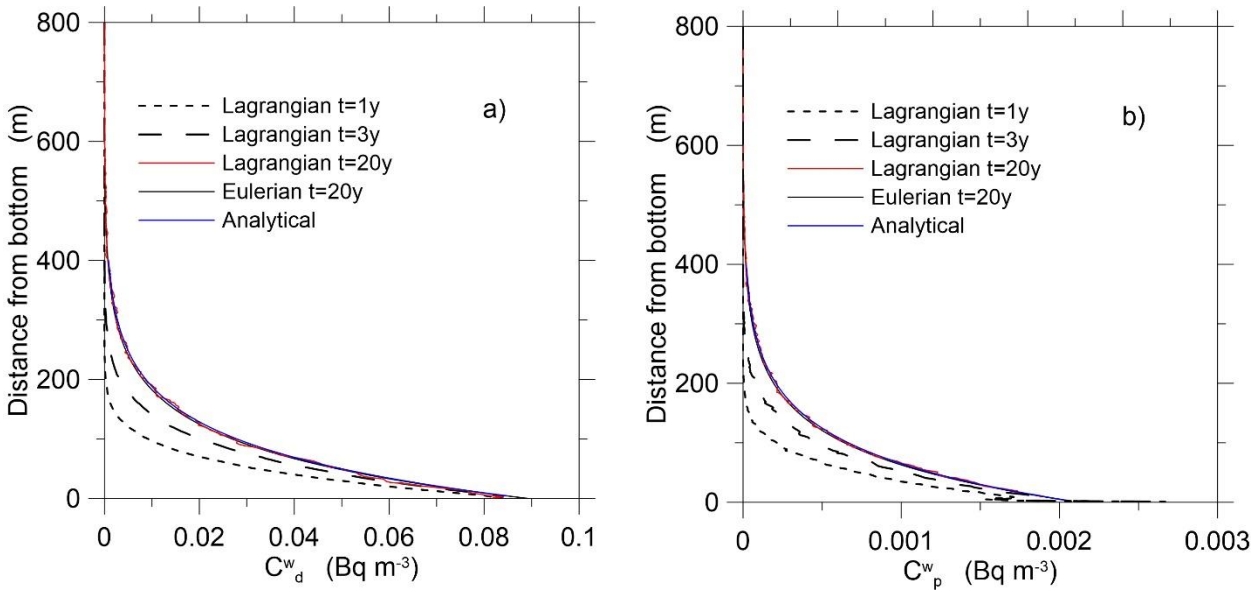

Figure 5: Equilibrium dissolved (a) and particulate (b) concentration profiles of ^{239,240}Pu. Dashed lines show Lagrangian model results after one and three years of simulation.

The thickness of the interface layer was chosen from the analysis of the root mean square error (RMSE) of the Lagrangian numerical solution from the analytic solution. We varied ΔZ, the number of particles, and time step to estimate the optimal value ΔZ. As seen in Fig. 6 at any time steps and number of particles, the RMSE first decreases with increasing thickness ΔZ, reaching a minimum at $\Delta Z \approx 5$m, and then increasing again. An increase in the number of particles and a decrease in the time step significantly reduces RMSE only at relatively small values ΔZ. This behaviour of RMSE can be explained by the fact that, at a small thickness of the transition layer ΔZ, a significant part of the particles are reflected from the bottom boundary, while at large thicknesses, the condition of the uniform distribution of concentration in this layer is significantly violated.

The optimal range of ΔZ can be estimated using numerical parameters. The ΔZ must be greater than the maximum vertical displacement of the particle during the one time step to satisfy the condition that the particle cannot jump over this layer during the one time step. On the other hand, ΔZ must be small enough to approximate uniform distribution of concentration in this layer. Therefore, the optimal range is defined from the relation

$$W_{p,\max}\Delta t + \sqrt{6K_V \Delta t} << \Delta Z << l_c, \tag{41}$$

where $W_{p,\max}$ is maximal settling velocity, $l_c = \bar{C}_d^w / \left|\partial \bar{C}_d^w / \partial z\right|$ is the characteristic length scale of the averaged in the interface layer concentration profile.

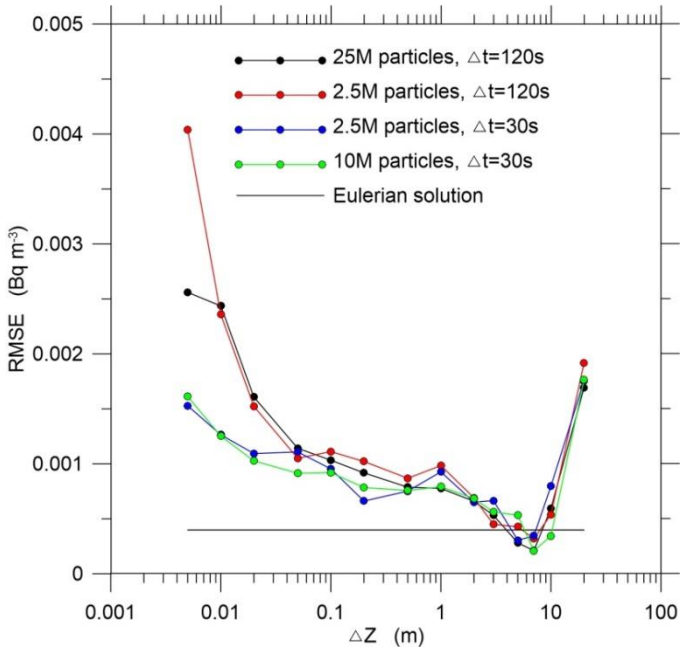

Figure 6: Dependence of root-mean standard error (RMSE) of concentration on the thickness of the interface layer ΔZ , number of particles, and time step Δt .

The studies of the accuracy of particle methods (Büyükçelebi et al., 2021; Graham, Moyeed, 2002) help choosing the appropriate number of particles to achieve the required accuracy, whereas effects of grid spacing, number of particles, and interpolation were considered by Perianez et al. (2023). Our study showed that choosing the appropriate time step and thickness of the near-bottom water layer for particular problems can be more significant for the resulting accuracy of the simulation than the number of particles.Results of simulations shown in Fig 5 and Fig 6 were obtained using MPI-based parallel computing on 20 cores of Intel(R) Xeon(R) Platinum 8268 CPU 2.90GHz power station. During the heaviest scenario with 25M particles, it used 140MB RAM and the calculation time was around 3 hours. Each independent MPI process was initialized with different random seeds for the random generator and calculated concentrations were summarized over all processed before every output record.

5. Conclusions

In the study, the particle-tracking method for the transport of radionuclides in multicomponent ocean medium (water and multifractional suspended and deposited sediments) is considered using a probabilistic approach for simulating processes of interaction between several states of radioactivity. Three novel approaches were developed and implemented in code. Firstly, the state transformations in the result of reactions of the first order were described using the master equation for the probability of the particle being in the given state. Expanding the solution of this matrix equation in a series of powers $r_{\alpha\beta}\Delta t$ and restricting ourselves to first-order terms (Euler approximation), we obtained the solution at the next time step. This approach can be applied to any linear system of equations describing phase transitions with any number of states. However, it requires small values of the transition probabilities to ensure only a single phase change during the time step. The evolution of the particle position in the state α during the time step consists of deterministic displacement, and displacement by uncorrelated random walk. Secondly, we developed a new approach to the interface conditions between the water column and bottom sediment. Fluxes through the bed surface in terms of Lagrangian particles correspond to a particle state change. Therefore, bottom boundary conditions can be considered as the reaction terms in transport equations. For this purpose, we introduced a thin near-bottom interface layer of thickness ΔZ where boundary conditions are converted into source terms. The corresponding master equation for the transition probabilities was derived for this layer. It was shown that the proposed approach can efficiently reproduce the correct boundary conditions which was evaluated by comparison with an analytical and numerical solution for the scavenging particular case. Thirdly, we showed that the optimal thickness of the interface layer must be greater than the maximum vertical displacement of the particle during the one-time step, but it must be small enough to satisfy the condition of uniform distribution of concentration in this layer.

The proposed probabilistic approach for simulating processes of interaction between states of contaminant is simple and effective for any number of states. It has already been used to simulate the hypothetical releases of ^{137}Cs from four nuclear power plants placed in the Bohai, Yellow, and East China Seas (Brovchenko et al., 2022) where the bottom component was about 40% of dissolved ^{137}Cs.

6. Appendix A. Constant A

$$A=\left[2K_V^2k_2^2\left(k_1+k_2\right)^3\right)\gamma^2\left(-1+\sqrt{1+4\gamma}\right)\theta W_{pw}\Big]\Big/Denom,$$

$$
\begin{aligned}
Denom = &\left\{-4K_V^2k_2^2\left(k_1+k_2\right)^3\gamma^3\theta W_{pw}-2K_Vk_1k_2\left(k_1+k_2\right)\gamma\theta\left[2K_{V^2}\left(k_1+k_2\right)^2\gamma^2+\right.\right.\\
&\left.k_1\left(-1-2\gamma+\sqrt{1+4\kappa}\right)W_p^2\right\}W_{pw}+\varepsilon k_2\theta\left(1-\sqrt{1+4\gamma}\right)\\
&\left[k_1^3\left(-1-2\gamma+\sqrt{1+4\gamma}\right)W_p^4+2K_Vk_1\gamma^2W_p\left(k_1+k_2\right)^2\left(k_1W_p+k_2W_{pw}\right)\right]Z_*+\\
&k_1\left(1-\sqrt{1+4\gamma}\right)W_p\left[k_1^2W_p^3\left(-1-2\gamma+\sqrt{1+4\gamma}\right)\left(W_{pw}-\left(1-\varepsilon\right)k_2K_d\rho_s\theta Z_*\right)+\right.\\
&\left.\left.2K_V\left(k_1+k_2\right)^2\gamma^2\left[k_1W_pW_{pw}-(1-\varepsilon)k_2K_d\rho_s\theta\left(k_1W_p+k_2W_{pw}\right)Z_*\right]\right\}\right.
\end{aligned}
$$

7. Acknowledgments

The research is supported by the National Research Foundation of Ukraine project no. 2020.02/0048, the European Union's Horizon 2020 research and innovation framework program (PolarRES, Grant Agreement 101003590), and the Korea Institute of Marine Science & Technology Promotion (KIMST) funded by the Ministry of Oceans and Fisheries (RS-2023-00256141). We are most grateful to Roman Bezhenar for the comments and suggestions that allowed us to improve the manuscript.

Code availability section

Name of the code: LagrRadBC

Contact: ibrovchenko@gmail.com

Hardware requirements: laptop for small, synthetic examples; workstation or cluster for realistic scenarios with MPI support

Program language: Fortran 90

Software required: Intel Fortran Compiler v12, MSMPI

Program size: 20KB

The source codes are available for download at the link: https://github.com/IBrovchenko/LagrProb/

References

Boudreau., B.P., 1997. Diagenetic models and their implementation: modelling transport and reactions in aquatic sediments. Springer-Verlag, Berlin, Heidelberg

Brovchenko, I., Kim, K.O., Maderich, V., Jung, K.T., Bezhenar, R., Ryu, J.H., Min, J.E., 2022. Sediment and radioactivity transport in the Bohai, Yellow, and East China Seas: A modelling study. Journal of Marine Science and Engineering 10, 596. https://doi.org/ 10.3390/jmse10050596

Büyükçelebi, B., Karabay, H., Bilgili, A. 2021. Exchange characteristics of an anthropogenically modified lagoon: an Eulerian-Lagrangian modeling case study with an emphasis on the number of particles. Journal of Environmental Engineering and Landscape Management. 29. 251-262. . https://doi.org/ 10.3846/jeelm.2021.15237.

Chapra S. 1997. Surface water-quality modeling. McGraw-Hill

Fletcher, C. A. J., 1991. Computational Techniques for Fluid Dynamics, 1. Fundamental and General Techniques. Springer Series in Computational Physics. 2nd edition Springer-Verlag, New York Berlin Heidelberg https://doi.org/10.1007/978-3-642-97035-1

Graham, D., Moyeed, R., 2002. How many particles for my Lagrangian simulations?, Powder Technology, 125, 179-186

Hunter, J., Craig, P., Phillips, H., 1993. On the use of random walk models with spatially variable diffusivity. Journal of Computational Physics, 106 (2), 366–376. http://dx.doi.org/10.1016/S0021-9991(83)71114-9

Kinzelbach, W.,1987. The random-walk method in pollutant transport simulation. In: Custodio E et al (eds) Advances in analytical and numerical groundwater flow and quality modelling. D. Reidel, Norwell, 227–246.

Kehl C., Nooteboom, P. D., Kaandorp, M.L.A., van Sebille, E., 2023. Efficiently simulating Lagrangian particles in large-scale ocean flows--Data structures and their impact on geophysical applications. Computers & Geosciences 175, 105322. https://doi.org/10.1016/j.cageo.2023.105322

Kloeden, P.E., Platen, E. 1992. Numerical solution of stochastic differential equations. Springer, Berlin.

Livingston, H. D., Povinec, P. P., Ito, T., Togawa, O., 2001. The behavior of plutonium in the Pacific Ocean. In: Kudo, A. (Ed.), Plutonium in the Environment, Radioactivity in the Environment. Elsevier, 267-292. doi.org/10.1016/S1569-4860(01)80019-X

Lynch, D.R., Greenberg, D.A., Bilgili, A., Mcgillicuddy, D.J., Manning, J.P., Aretxabaleta, A.L., 2015. Particles in the Coastal Ocean. Theory and Applications. Cambridge University Press, NY.

Maderich V., Jung K.T., Brovchenko I., Kim K.O., 2017. Migration of radioactivity in multi-fraction sediments. Environmental Fluid Mechanics, 17(6), 1207-1231, https://doi: 10.1007/s10652-017-9545-9.

Maderich, V., Kim, K. O., Brovchenko I., Kivva S. Kim H., 2021. Scavenging processes in multicomponent medium with first-order reaction kinetics: Lagrangian and Eulerian modeling. Environmental Fluid Mechanics, 21, 817–842. https://doi.org/10.1007/s10652-021-09799-1

Maderich, V., Kim, K.O., Brovchenko, I, Jung, K.T., Kivva, S., Kovalets, K., 2022. Dispersion of particle-reactive elements caused by the phase transitions in scavenging. Journal of Geophysical Research, 127, e2022JC019108. https://doi.org/10.1029/2022JC019108.

Periáñez, R., 2020. Models for predicting the transport of radionuclides in the Red Sea. Journal of Environmental Radioactivity, 203-204, 106396. http://dx.doi.org/10.1016/j.jenvrad.2020.106396.

Periáñez, R., Elliot, A. J., 2002. A particle-tracking method for simulating the dispersion of non-conservative radionuclides in coastal waters. Journal of Environmental Radioactivity, 58, 13–33.

Periáñez, R., Bezhenar, R., Brovchenko, I., Jung, K.T., Kim, K.O., Maderich, V., 2018. The marine k_d and water/sediment interaction problem. Journal of Environmental Radioactivity 192, 635–647.

Periáñez R., Bezhenar R., Brovchenko I., Duffa C., Iosjpe M., Jung K.T., Kim K.O., Kobayashi T., Liptak L., Little A., Maderich V., McGinnity P., Min B.I., Nies H., Osvath I., Suh K.S., de With G., 2019. Marine radionuclide transport modelling: Recent developments, problems and challenges. Environmental Modelling and Software, 122, 104523, https://doi.org/10.1016/j.envsoft.2019.104523.

Periáñez, R., Brovchenko, I., Jung, K.T., Kim, K. O., Kobayashi T., Liptak L., Little, A., Maderich, V., Min, B. I., Suh, K. S., 2023. Some considerations on the dependence to numerical schemes of Lagrangian radionuclide transport models for the aquatic environment. Journal of Environmental Radioactivity, **261**, 107138 https://doi.org/10.1016/j.jenvrad.2023.107138

van Rijn, L.C., 1984. Sediment transport, Part II: Suspended load transport. Journal of Hydraulic Engineering 110, 1613- 1641.

van Sebille, E, Griffies, S.M., Abernathey, R., Adams, T.P., Berloff, P., Biastoch, A, Blanke, B., Chassignet, E.P., Cheng, Y., Cotter, C.J., Deleersnijder, E., Döös, K., Drake, H.F., Drijfhout, S., Gary, S.F., Heemink, A.W., Kjellsson, J., Koszalka, I.M., Lange, M., Lique, C., MacGilchrist, G.A., Marsh, R., Mayorga Adame, C.G., McAdam, R., Nencioli, F., Paris, C.B., Piggott, M.D., Polton, J.A., Rühs, S., Shah, S.H., Thomas, M.D., Wang,

J., Wolfram, P.J., Zanna, L., Zika, J.D., 2018. Lagrangian ocean analysis: fundamentals and practices. Ocean Modelling, 121, 49-75.. http://dx.doi.org/10.1016/j.ocemod.2017.11.008

Winterwerp, J.C., van Kesteren, W.G., 2004. Introduction to the physics of cohesive sediment in the marine environment. Developments in Sedimentology Series, 56. Elsevier, Amsterdam, Netherlands.

List of Figures